

Ce,Tb-Doped Y_2SiO_5 Phosphor Luminescence Emissions Modeling and Simulation

D. Cervantes, D.L. Flores, E. Gutiérrez and M.A. Chacón

Abstract White light-emitting diodes offer the possibility of efficient, safe, and reliable solid-state lighting, and thus have various applications in artificial lighting. Reported white light-emitting phosphors usually contain rare-earth metals and are generally prepared by high-energy processes. The purpose of this research is the modeling and simulation of the molar percentages of cerium and terbium required to be incorporated into a yttrium silicate ($Y_2SiO_5:Ce,Tb$) crystal structure for luminescent emission. The input data used for the modeling process comes from experiments with a set of molar concentrations of cerium and terbium ranging from 0.5 to 2%, and, from 1 to 6%, respectively; chromaticity coordinates are obtained from the photoluminescence spectra generated by the luminescent materials. With the information above, a simulation based on the proposed mathematical model was performed in order to obtain the approximation of the luminescent response of the molar concentrations whose experiments were not carried out in the laboratory. To demonstrate the results of the model and its simulation, a tool developed in the agent-based platform NetLogo is presented, which allows the user to observe the trend of the chromaticity coordinates for different molar percentages of cerium and cerium into yttrium silicate crystal structures.

Keywords Rare-earth phosphors materials · Chromaticity coordinates · Simulation · NetLogo

D. Cervantes · D.L. Flores (✉) · E. Gutiérrez · M.A. Chacón
Autonomous University of Baja California, Ensenada, Mexico
e-mail: dflores@uabc.edu.mx

D. Cervantes
e-mail: dcervantes42@uabc.edu.mx

E. Gutiérrez
e-mail: everardo.gutierrez@uabc.edu.mx

M.A. Chacón
e-mail: marco.chacon@uabc.edu.mx

1 Introduction

In the last few decades there has been a great deal of interest in white light sources based on rare-earth doped phosphor materials due to their potential range of applications, for example, in the field of full color displays and solid state lighting. It is well known that white light is generated by an adequate blend of the three primary colors (such as red, green and blue). The selection of phosphor materials depends on the activation energy matching or the coupling of phosphor materials. In addition, it is necessary to increase the efficiency of white light-emitting solid state devices, so special attention has been paid lately to the development of new phosphors that can be activated in the range of long-UV ($\lambda = 300\text{--}420$ nm) and/or blue radiation [1–3]. This consequently results in lower power consumption, which positively impacts the environment by reducing greenhouse gases emissions and the elimination of mercury in solid-state lamps production [4].

The use of one or two rare earth (RE) ions as color centers in the same crystalline host has been tested as an option for the development of new phosphor materials. Ce-doped Y_2SiO_5 has proven to be an excellent blue-emitting phosphor, while Tb-doped Y_2SiO_5 is appropriate for light emission in the green region [5, 6]. However, when both RE ions are incorporated in the same host matrix, Ce^{3+} becomes a blue broadband emitter with the ability of transferring energy from its lowest 5d levels to Tb^{3+} ions [1, 2, 7–9]. Due to this energy transfer it is possible to obtain both rare-earth emission simultaneously with only one excitation wavelength in the low energy region of UV radiation. Moreover, laboratory experiments can be complemented with computational tools, that is, from the first experimental results design laboratory experiments aimed to specific targets within the range possible results.

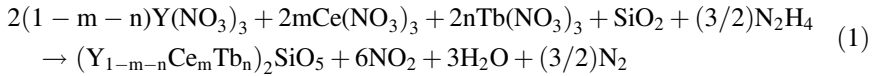
The present work analyses the chromaticity coordinates tendency of a series of cerium and terbium coactivated yttrium silicate phosphors with different rare-earth ions molar percentages. The chromaticity coordinates were determined using the emission spectra obtained by the photoluminescence technique and the CIE standard equations of primary colors with the uses of the NetLogo software to correlate the cerium and terbium molar percentages and then obtain the regression equation to design experiments with the optimum rare-earth ions molar percentages to reach the closest chromaticity coordinates with the D65 white light or to obtain specific chromaticity coordinates in the path of cerium and terbium simultaneous emission.

2 Experimental

The purpose of this work is to design experiments using computational resources and some experimental data obtained from luminescent properties of the system $\text{Y}_2\text{SiO}_5:\text{Ce},\text{Tb}$ at different rare-earth molar percentages from 0.5 to 2 and from 1 to 6 for cerium and terbium ions, respectively. The goal is to reduce the number of laboratory experiments to achieve specific luminescent properties.

2.1 Synthesis of Cerium and Terbium Activated Yttrium Silicate, YSO:Ce,Tb

The synthesis of the YSO:Ce,Tb phosphor system was made by the pressure-assisted combustion synthesis (PACS) method [10, 11] according to the following chemical reaction:



Details of synthesis procedures were described in a previous publication in Cervantes et al. [12].

2.2 Characterization

Emission spectra were measured with a fluorescence spectrophotometer (PL, HITACHI f-7000) using 355 nm as excitation wavelength. Emission spectra data was used to determine the chromaticity coordinates through the NetLogo software and the design of a program that uses the CIE 1931 standard equations. The crystallographic structure of the nanoparticles was determined by X-ray diffraction (XRD, PHILIPS X' Pert) using Cu-K_a radiation. Morphology images of the resulting powders were obtained by transmission electron microscopy (TEM, JEOL 2010).

3 Proposal Model

A simulation model is proposed as shown in Fig. 1; this figure depicts that the emission spectra that are provided to the simulation comes from experiments conducted in the laboratory described in [12]. Using our software simulation proposal in Netlogo, the chromaticity coordinates for each of the emission spectra of the materials were simulated and the values are shown in Table 1.

Once having the chromaticity coordinates, which according to CIE1931 (D65) are (0.3128, 0.329), the Euclidean distance to the coordinates of white light is calculated, with the data shown in Table 2.

With the values of the distances an equation multivariate linear regression obtained, where independent variables are the molar concentration of cerium and terbium and the dependent variable is the Euclidean distance. A linear least square approach was used as regression method, and its high level algorithms is as follows [13, 14]:

Fig. 1 Proposal model diagram for rare-earth molar concentration simulation

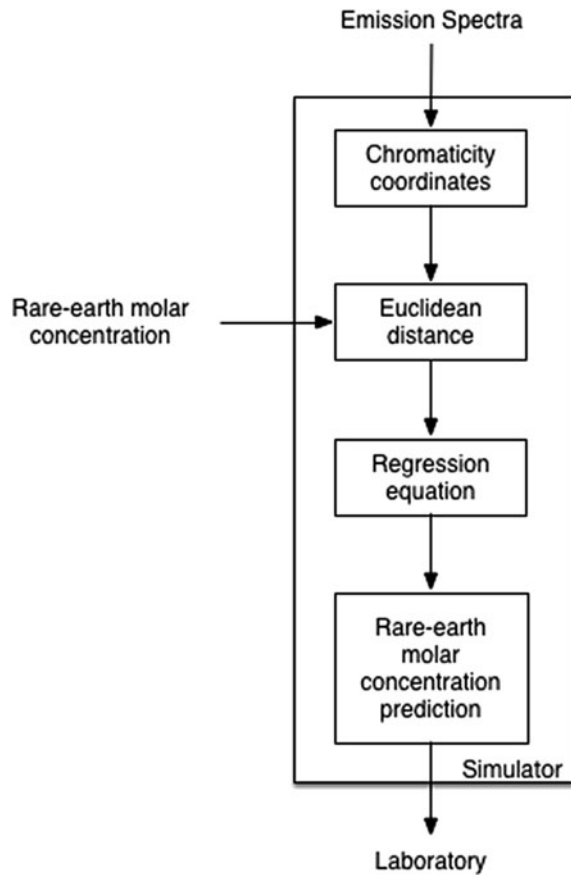


Table 1 Chromaticity coordinates of each of nanomaterials

Name	Cerium (mol%)	Terbium (mol%)	Coord X (CIE1931)	Coord Y (CIE1931)
YSO0.5-3	0.5	3	0.2320	0.2656
YSO0.75-1	0.75	1	0.1793	0.1500
YSO0.75-2	0.75	2	0.2057	0.2143
YSO0.75-3	0.75	3	0.2312	0.2564
YSO0.75-3.5	0.75	3.5	0.2405	0.2929
YSO0.75-4	0.75	4	0.2440	0.3080
YSO0.75-4.96	0.75	4.96	0.2592	0.3407
YSO0.75-5	0.75	5	0.2585	0.3348
YSO0.75-6	0.75	6	0.2702	0.3631
YSO1-3	1	3	0.2323	0.2617
YSO2-3	2	3	0.2350	0.2802

Table 2 Euclidean distance of each of the nanomaterials

Name	Euclidean distance
YSO0.5-3	0.102704430
YSO0.75-1	0.223300806
YSO0.75-2	0.156928328
YSO0.75-3	0.109221426
YSO0.75-3.5	0.080811509
YSO0.75-4	0.071933580
YSO0.75-4.96	0.054608882
YSO0.75-5	0.054862100
YSO0.75-6	0.054567115
YSO1-3	0.104926355
YSO2-3	0.091838336

Algorithm 1. Regression with Linear Least Square

Input: A set of m linear equations, each one with n independent variables and one dependent variable, given by the previous set of experiments.

Step 1. State each input equation as: $f(x; \beta) = \beta_0 + \beta_1 x_1 + \dots + \beta_n x_n$. Where each independent variable (x_1, x_2, \dots, x_n) represent the used rare earths ions and the estimated $f(x; \beta)$ values are given by results of the input experiments.

Step 2. Use quadratic minimization to find the coefficients $\beta_0, \beta_1, \dots, \beta_n$ setting the system in matrix equation of the type $Ax = b$ with the formula: $(A^T A)\beta = A^T y$

Step 3. Calculate from previous formula the estimated slope and coefficients for independent variables and report them as output.

This algorithm gave as a result a set of coefficients, as shown in the following equation:

$$EuclDist = 0.233 - 0.0199 * Ce - 0.0330 * Tb \quad (2)$$

With the standard deviation is 0.0223565 and adjusted R^2 is 80.7 %.

Also a multivariate quadratic regression was performed, which is shown in the following equation:

$$EuclDist = 0.316 - 0.00906 * Ce - 0.0943 * Tb + 0.00864 * Tb^2 \quad (3)$$

in this regression, the standard deviation is 0.00323709 and the adjusted R^2 is 99.6 %.

Once these equations are obtained, a table with a series of experiments designed to perform in the laboratory as required by the expert can be generated. This set of suggested experimental values were calculated with a modified bisection search as follows [15]:

Algorithm 2. Bisection Search

Input: An interval $[a, b]$ for one of the rare earths (cerium, terbium) and the factors c_1 and c_2 to calculate the cost function $f = c_1 \text{ Cerium} + c_2 \text{ Terbium}$.

Step 1. Calculate the middle point of the interval $c = \frac{(a+b)}{2}$.

Step 2. For each value a , b and c , calculate the value for the dependent rare earth based on the linear equation given by the linear regression results.

Step 3. Calculate the cost function for (a, x_1) , (b, x_2) and (c, x_3) , using a , b and c as values for the independent rare earth and x_1 , x_2 and x_3 the calculated values in Step 2.

Step 4. If the convergence is satisfactory then return the pair (c, x_3) as proposed concentrations of rare earths to be tested experimentally and stop iterating.

Step 5. Replace either the lower or upper interval limit with c according with the cost function results, where our goal is to minimize it, and return to Step 1.

4 Results and Discussion

4.1 Emission Spectra and Crystalline Structure

The emission spectra of YSO:Ce,Tb nanopowders revealed the typical light emissions of the Ce^{3+} and Tb^{3+} ions (Fig. 2), revealing a broadband emission, located in the 380–475 nm wavelength range, which is generated by the 5d–4f

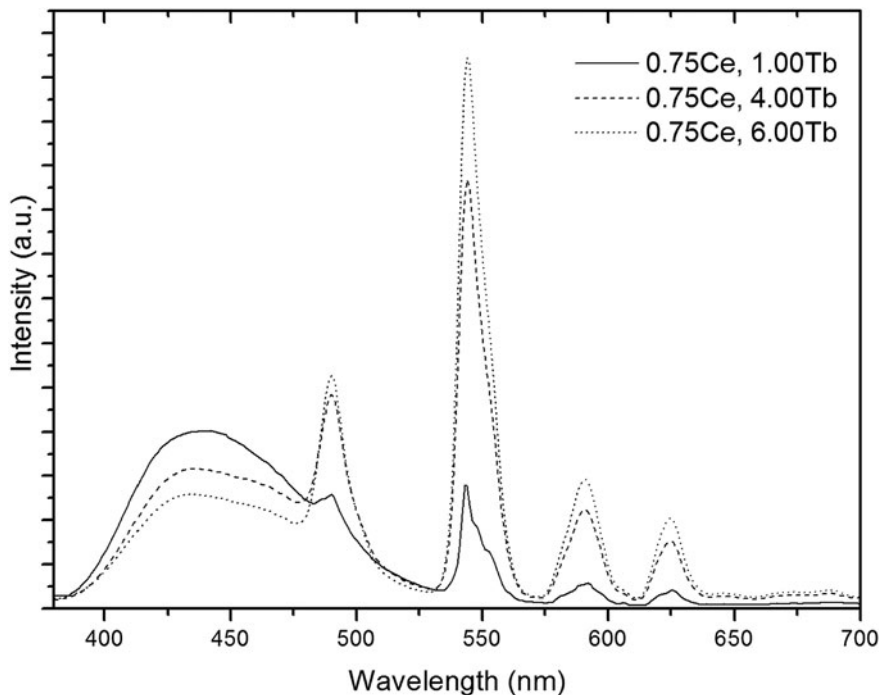


Fig. 2 Photoluminescence emission spectra of $\text{Y}_2\text{SiO}_5\text{:Ce,Tb}$ phosphors nanopowders

electronic transitions within the Ce^{3+} ions and a well-defined green emission located at 546 nm due to $^5\text{D}_4\text{-}^7\text{F}_5$ transitions in the Tb^{3+} ions. The emission peaks observed at 490, 591 and 624 nm are also associated to $^5\text{D}_4\text{-}^7\text{F}_6$, $^5\text{D}_4\text{-}^7\text{F}_4$ and $^5\text{D}_4\text{-}^7\text{F}_3$ transitions in Tb^{3+} ions, respectively. The chromaticity coordinates determined through emission spectra data show a linear trend that extends along the blue region to the green region in the CIE 1931 chromaticity coordinates diagram as a function of rare-earth ions molar percentages. These chromaticity coordinates were compared with chromaticity coordinates obtained by the color calculator software of the Osram Sylvania Company. Both sets of chromaticity coordinates had the same values. It is noteworthy that other authors have used Spectra Lux software to determine the chromaticity coordinates [16, 17]. Simultaneous emissions of Ce^{3+} and Tb^{3+} from $\text{YSO}:\text{Ce},\text{Tb}$ phosphors generates a light near to the chromaticity coordinates of D65 white-light. This light could get even closer to the D65 white light chromaticity coordinates with the addition of a red-emitting ion within the same host, or even more simple by mixing the $\text{YSO}:\text{Ce},\text{Tb}$ phosphor with a second phosphor compound, of red emission.

X-ray diffraction patterns (Fig. 3) of $\text{YSO}:\text{Ce},\text{Tb}$ nanopowders showed $\text{X1-Y}_2\text{SiO}_5$ crystal phase (JCPDS 41-0004 card) and correspond to a monoclinic

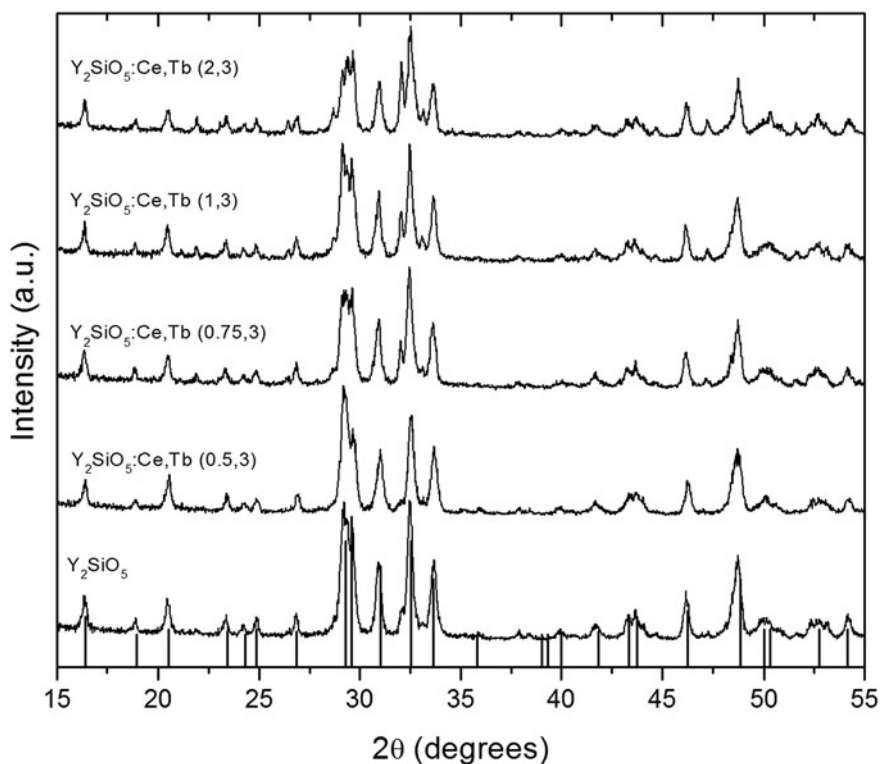


Fig. 3 XRD patterns of $\text{YSO}:\text{Ce},\text{Tb}$ nanopowders at different rare-earth molar percentages compared with the JCPDS card 41-0004 for $\text{X1-Y}_2\text{SiO}_5$ crystalline phase

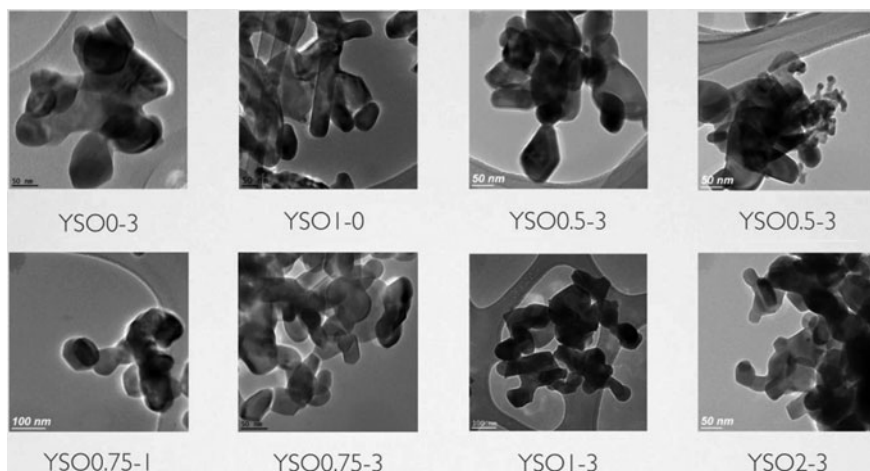


Fig. 4 TEM images of YSO:Ce,Tb powders at different rare-earth ions molar percentages

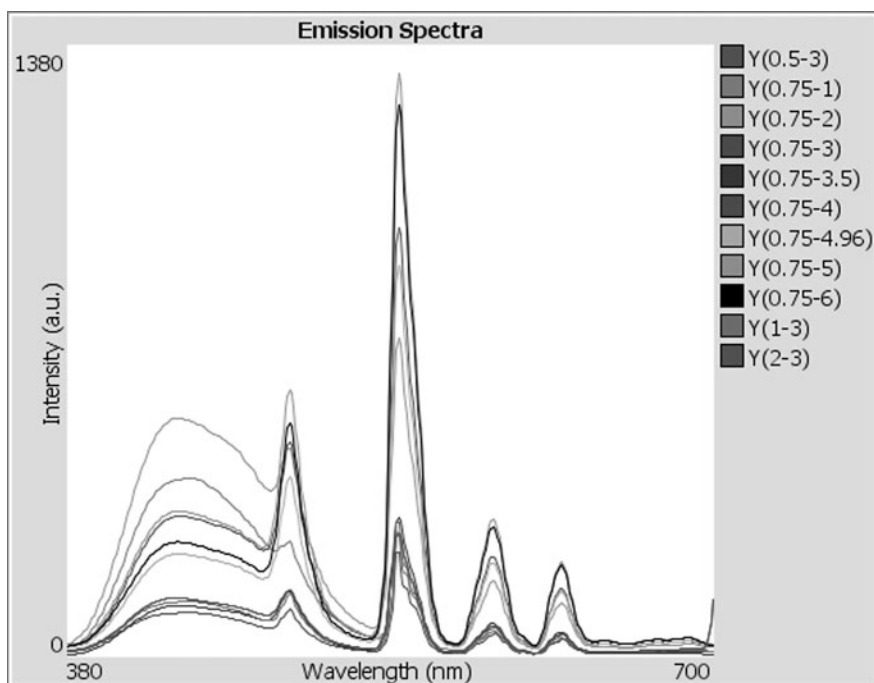


Fig. 5 Emission spectra of the $Y_2SiO_5:Ce,Tb$

system in accordance with the crystallographic phases found by other authors [18, 19]. The crystal structure was kept for the different rare-earth ions percentages. Figure 4 shows TEM images of YSO:Ce,Tb phosphors synthesized at different rare-earth ions molar percentages. Particles sizes of different samples were in the range from 30 to 100 nm.

4.2 An Agent-Based Platform for Data Analysis

A new tool was developed in an agent-based platform NetLogo, which allows the user to analyze the experimental data. Given a set of molar concentrations with their respective emission spectra, the platform allows visualizing emission spectra. It also calculates and shows on CIE 1931 chromaticity diagram the trend of the chromaticity coordinates for the different molar percentages of cerium and terbium.

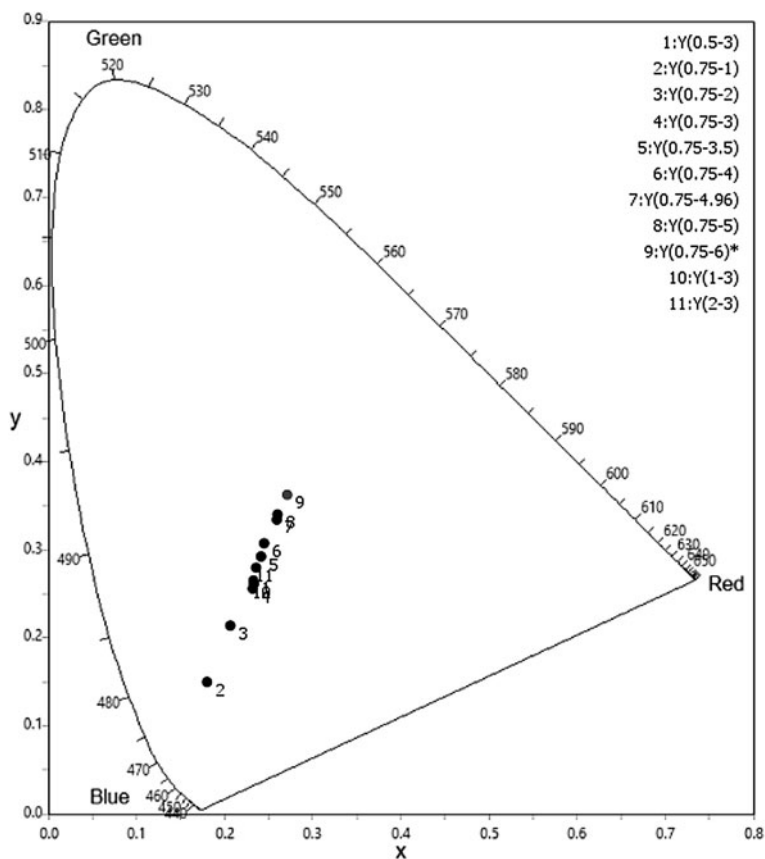


Fig. 6 Chromaticity coordinates of Y_2SiO_5 doped, on CIE 1931 chromaticity diagram

Figure 5 shows the emission spectra of the $Y_2SiO_5:Ce,Tb$ doped as presented by the platform. The x, y color chromaticity coordinates of the $Y_2SiO_5:Ce,Tb$ doped Yttrium Silicate have been determined and presented in Table 1 along with the x, y color chromaticity coordinates of the reported Y_2SiO_5 doped systems. Figure 6 presents the location of the chromaticity coordinates of Y_2SiO_5 doped on CIE 1931 chromaticity diagram. It is observed that, the chromaticity coordinates seem to have almost linear behavior.

The final analysis step allowed in the proposed platform gives the user some molar percentages as suggested for future experiments. First, Algorithm 1 is used to perform a linear regression over the input data, with molar concentrations and Euclidean distance as system variables. After that, Algorithm 2 allows to find some molar concentrations that minimize the cost function. This procedure needs to select the new concentrations without actually performing the experiments to calculate the chromaticity coordinates for each new combination. A function based on market costs was proposed as optimization criterion, the cerium concentration was multiplied by a weight of 0.14, while the terbium one by 0.86. Figure 7 shows the platform interface with the results for input data over Y_2SiO_5 doped with cerium and terbium, while Table 3 shows the molar percentages proposed by the platform.

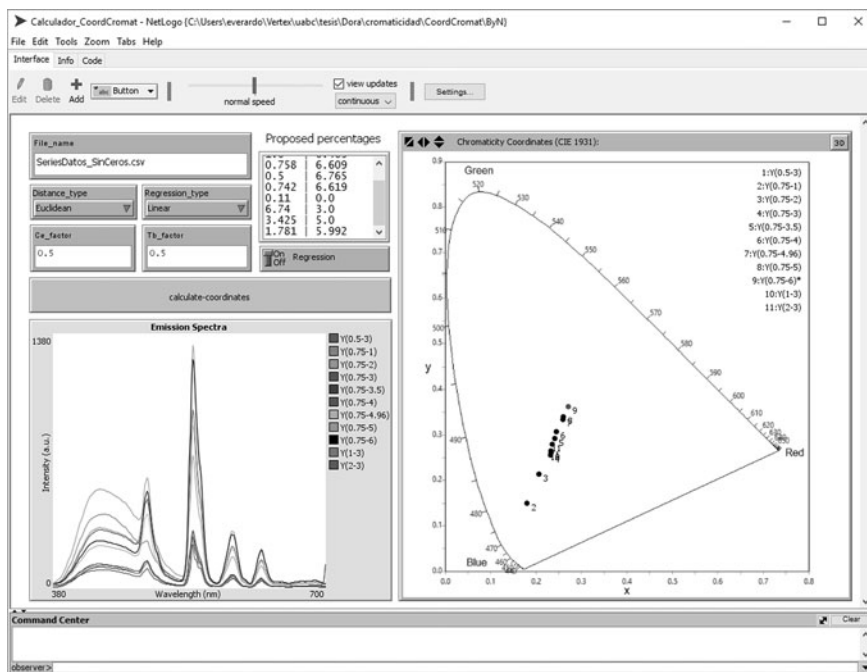


Fig. 7 NetLogo based platform interface

Table 3 Molar percentages proposed by the platform

Cerium	Terbium
1.0	6.463
0.758	6.609
0.5	6.765
0.742	6.619
6.74	3.0
3.425	5.0
2.596	5.5

5 Conclusions

The simultaneous emission of cerium and terbium in the yttrium silicate, which produce white light, approaches the D65 light.

A model prediction molar percentage of rare earth cerium and terbium in the yttrium silicate was created for greater approximation to the D65 white light and decrease the number of experiments in the laboratory.

The graphical interface in NetLogo, which helps to display the emission spectra and chromaticity, coordinates of the experimental data jointly it, was developed.

The tool produces a list of molar concentrations of rare earth that binds the set of experiments performed in the laboratory.

Acknowledgments The authors are grateful to G.A. Hirata for their invaluable support, and to E. Aparicio and F. Ruiz for technical assistance.

References

- Ballato J, Lewis JS III, Holloway P (1999) Display applications of rare-earth-doped materials. *MRS Bull.* doi:[10.1557/S0883769400053070](https://doi.org/10.1557/S0883769400053070)
- Gonzalez-Ortega JA, Tejada EM, Perea N, Hirata GA, Bosze EJ, McKittrick J (2005) White light emission from rare earth activated yttrium silicate nanocrystalline powders and thin film. *J Opt Mater* 27:1221–1227
- Mingming X, Yunbei MA, Xixian L, Yao F, Tao J, Hong W, Xiaolong D (2014) Design and achieving of multicolor upconversion emission based on rare-earth doped tellurite. *J Rare Earths* 32:394–398
- Gouveia-Neto AS, Rios NPSM, Bueno LA (2012) Spectroscopic study and white-light simulation using praseodymium-doped fluorogermanate glass as single phosphor for white LEDs. *J Opt Mater* 35:126–129
- Shin SH, Jeon DY, Suh KS (2001) Emission band shift of the cathode luminescence of Y_2SiO_5 :Ce phosphor affected by its activator concentration. *Jpn J Appl Phys* 1 40:4715–4719
- Choi YY, Sohn K, Park HD, Choi SY (2001) Luminescence and decay behaviors of Tb-doped yttrium silicate. *J Mater Res* 16:881–889
- Bosze EJ, Carver J, Singson S, McKittrick J, Hirata GA (2007) Long-ultraviolet-excited white-light emission in rare-earth-activated yttrium-oxyorthosilicate. *J Amer Cer Soc.* doi:[10.1111/j.1551-2916.2007.01809.x](https://doi.org/10.1111/j.1551-2916.2007.01809.x)

8. Ghosh P, Kar A, Patra A (2010) Energy transfer study between Ce^{3+} and Tb^{3+} ions in doped and core-shell sodium yttrium fluoride nanocrystals. *J Nanoscale* 2:1196–1202
9. Kar A, Patra A (2012) Impacts of core-shell structures on properties of lanthanide-based nanocrystals: crystal phase, lattice strain, downconversion, upconversion and energy transfer. *J Nanoscale* 4:3608–3619
10. García R, Hirata GA, McKittrick J (2001) New combustion synthesis technique for the production of $(In_xGa_{1-x})_2O_3$ powders: hydrazine/metal nitrate method. *J Mater Res* 16:1059–1065
11. Hirata GA, Perea N, Tejada M, Gonzalez-Ortega JA, McKittrick J (2005) Luminescence study in Eu-doped aluminum oxide phosphors. *J Opt Mater* 27:1311–1315
12. Cervantes-Vásquez D, Contreras OE, Hirata GA (2013) Quantum efficiency of silica-coated rare-earth doped yttrium silicate. *J Lumin* 143:226–232
13. Lawson CL, Hanson RJ (1974) Solving least squares problems. Prentice-Hall, Englewood Cliffs
14. NIST/SEMATECH e-Handbook of Statistical Methods. <http://www.itl.nist.gov/div898/handbook/>. Accessed 01 July 2015
15. Burden RL, Faires JD (1985) Numerical analysis. Thomson, USA
16. Gomes J, Serra OA (2008) Cerium-based phosphors: blue luminescent properties for applications in optical displays. *J Mater Sci* 43:546–550
17. Maia AS, Stefani R, Kodaira CA, Felinto MCFC, Teotonio EES, Brito HF (2008) Luminescent nanoparticles of $MgAl_2O_4:Eu, Dy$ prepared by citrate sol-gel method. *J Opt Mat* 31:440–444
18. Saha S, Chowdhury P, Patra A (2005) Luminescence of Ce^{3+} in Y_2SiO_5 nanocrystals: role of crystal structure and crystal size. *J Phys Chem B* 109:2699–2702
19. Ghosh P, Sadhu S, Patra A (2006) Preparation and photoluminescence properties of $Y_2SiO_5:Eu^{3+}$ nanocrystals. *J Phys Chem Chem Phys* 8:3242–3248